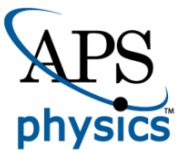

Intervalley energy of GaN conduction band measured by femtosecond pump-probe spectroscopy

Saulius Marcinkevičius, Tomas K. Uždavinys, Humberto M. Foronda, Daniel A. Cohen, Claude Weisbuch, and James S. Speck

Phys. Rev. B **94**, 235205 — Published 19 December 2016

DOI: 10.1103/PhysRevB.94.235205

Intervalley energy of GaN conduction band measured by femtosecond pump-probe spectroscopy

Saulius Marcinkevičius,[1,*] Tomas K. Uždavinys,[1] Humberto M. Foronda,[2] Daniel A. Cohen,[2] Claude Weisbuch,[2,3] and James S. Speck[2]

[1] *KTH Royal Institute of Technology, Department of Materials and Nano Physics, Electrum 229, 16440 Kista, Sweden*
[2] *Materials Department, University of California, Santa Barbara, California 93106, USA*
[3] *Laboratoire de la Physique de la Matière Condensée, CNRS, Ecole Polytechnique, Palaiseau, France*

(Dated: November 17, 2016)

Time-resolved transmission and reflection measurements were performed for bulk GaN at room temperature to evaluate the energy of the first conduction band satellite valley. The measurements showed clear threshold-like spectra for transmission decay and reflection rise times. The thresholds were associated with the onset of the intervalley electron scattering. Transmission measurements with pump and probe pulses in the near infrared produced the intervalley energy of 0.97 ± 0.02 eV. Ultraviolet pump and infrared probe reflection provided a similar value. Comparison of the threshold energies obtained in these experiments allowed estimating the hole effective mass in the upper valence band of $1.4m_0$. Modelling of the reflection transients with rate equations suggests that intra- and intervalley electron - LO phonon scattering times are about 30 fs and 8 fs, respectively.

PACS numbers: 71.20.Nr, 72.10.Di, 78.47.-p

I. INTRODUCTION

The energy difference between the lowest conduction band valleys is a fundamental semiconductor parameter affecting performance of electronic devices via the intervalley electron scattering. While for most of group IV and III-V semiconductors the intervalley energy (IVE) is well known, for GaN it is still disputed. Recent photoemission experiments produced IVE values of $0.90 - 0.95$ eV [1, 2]. Photoexcited field emission investigations yielded a value in the range $1.18 - 1.21$ eV [3]. These values are considerably smaller than energies > 2 eV obtained by *ab initio* calculations [4, 5].The high IVE values were supported by the interpretation of ellipsometric data [6, 7]. The discrepancy between the IVE values determined by different methods has revived discussion about this important band structure parameter [7].

In view of the mentioned IVE differences, a note on the interpretation of ellipsometric data is appropriate. While the assignment of peaks in the dielectric function spectra to transitions at critical points of the band structure can be done through symmetry arguments, assessment of transition strengths and comparison with similar materials [8], the determination of conduction band extrema requires additional inputs. First, for transitions between the upper valence band and the conduction band (in the spectral range from the band gap to ~ 20 eV), one needs to know the valence band dispersion. This dispersion is usually calculated by *ab initio* methods. From an agreement between the calculated interband transitions and ellipsometric data, one then deduces energies of higher conduction band potential minima that are, in fact, theoretically calculated. Second, one can analyse optical transitions observed by ellipsometry at higher energies, from 20 eV to 30 eV. In this spectral range, transitions take place between the Ga $3d$ valence band and the conduction band [6]. As the deep $3d$ valence band has no dispersion, transitions originating from this band directly measure the conduction band states. On the basis of such measurements, Rakel *et al.* [6] found a higher conduction band valley at ~ 1 eV above the lowest conduction band minimum. These high energy transitions, however, are strongly influenced by excitonic effects, which have to be taken into account in the IVE evaluation. In Ref. 6, the excitonic correction of 1 eV was invoked, placing the IVE at 2 eV. The correction was extrapolated from a 0.66 eV core exciton correction measured by Aspnes *et al.* [9] for the In $4d$ band in InAs. It should be remarked that applying the Ga $3d$ band core exciton correction of $0.1 - 0.2$ eV [9] would lead to the ellipsometric IVE of $1.1 - 1.2$ eV.

The IVE can also be determined by other optical experiments. Previously, optical studies of the IVE in GaN were performed by continuous wave (cw) high temperature photoluminescence (PL) [10], high field electroluminescence [11], and time-resolved transmission [12] and reflection [13]. Temperature dependent PL measurements suggested that the energy separation between the two lowest conduction band valleys at the Γ point is only 0.29 eV [10]. On the other hand, the study of electroluminescence from GaN/AlGaN high electron mobility transistors placed the IVE at 1.8 eV [11]. Here one should note that interpretation of cw luminescence experiments in terms of higher energy transitions is quite indirect, as they are seen under non-standard excitation conditions. Time-resolved optical measurements leave less space for ambiguities, since IVE evaluation is based on the energy dependent onset of the intervalley scattering, which slows down the electron relaxation to the bottom of the Γ valley and is directly observed in PL and pump-probe transients [14–16].

For GaN, two such experiments have been performed. Sun *et al.* measured differential transmission (DT) of

n-doped GaN by using near-infrared (NIR) pump and ultraviolet (UV) probe pulses [12]. In a "reverse" differential reflection (DR) experiment by Wu *et al.* [13], a UV pump pulse was used to excite electrons to energies around the intervalley scattering threshold, while the electron relaxation was monitored by a NIR probe pulse. In both cases, fundamental and third harmonic pulses from a wavelength tunable femtosecond laser were used; hence, the wavelengths of pump and probe pulses were tuned simultaneously. This affected the spectral region covered in Sun's DT experiment since the tuning range of the UV pulses was limited by the GaN band gap. Concerning Wu's UV pump and NIR probe DR experiment, evaluation of the IVE was inherently affected by the ambiguity of the valence band dispersion.

In this work, we have performed DT measurements with pump and probe pulses in the NIR. Such an experiment probes only states in the conduction band; hence, the determined IVE is not influenced by the uncertainty of the hole effective mass and its dependence on the $\boldsymbol{k}$ vector. These measurements were complemented by UV pump and NIR probe DR experiment using a much wider photon energy range compared to Ref. 13. Comparison of DT and DR results allowed assessing effective mass of the top most valence band. The experiments have been carried out on the same high quality unintentionally n-doped GaN bulk samples that, most likely, are of a considerably higher crystalline quality compared to those used in the early studies.

II. EXPERIMENT

In the wavelength-degenerate DT experiment, pulses from a Ti:sapphire laser (800 to 1030 nm central wavelength, 130 fs pulse duration, 80 MHz pulse repetition frequency) and an optical parametric oscillator (1100 to 1280 nm, 180 fs, 76 MHz) were used. The pump and probe pulse energies were $1 - 1.5$ nJ and $0.02 - 0.03$ nJ, respectively. The DT signal was weak and its transients short; therefore, precautions had to be taken to remove spurious contribution from the pump. To filter out the pump pulse photons scattered towards the detector, a Glan polarizer was placed in front the detector, and the linear pump pulse polarization was rotated by $\pi/2$ with a tunable wavelength $\lambda/2$ waveplate. Noise induced by the laser pulse intensity fluctuations was reduced by the balanced detection. Due to the weak free carrier absorption, the whole crystal contributes to the transmission change. Thus, it was important to maintain the spatial overlap of the non-collinear pump and probe beams throughout the whole sample thickness.

The DR experiments were carried out using Ti:sapphire laser pulses at third harmonic and fundamental wavelengths. The pump (probe) pulses of 150 (130) fs duration and 80 MHz repetition frequency were tuned from 255 (765) nm to 293 (880) nm. Due to the strong absorption of the UV pump pulse, the DR signal was generated in the top layer of the sample ($\sim$ 100 nm). The pump pulse power was scaled with the photon energy between 0.60 and 0.68 nJ, corresponding to an average photoexcited carrier density of 1×10^{18} cm^{-3}. For such carrier densities, hot carrier generation related to Auger recombination can safely be ignored [17].

All the measurements were performed at room temperature. The influence of the pump pulse on the probe pulse intensity was measured with a lock-in amplifier synchronized with a mechanical chopper modulating the pump beam. The pump and probe pulses were focused on a sample surface to spots of a about 100 and 20 μm in diameter, respectively.

Unintentionally n-doped ($\sim 3 \times 10^{17}$ cm^{-3}) c-plane high quality GaN single crystals, produced by Furukawa Co., Ltd. and Nanowin Technology Co. were studied. The sample thicknesses were 630 μm and 300 μm, respectively. The threading dislocation density determined by panchromatic cathodoluminescence (CL) imaging was 4.2×10^5 cm^{-2} for the Nanowin and 1.4×10^6 cm^{-2} for the Furukawa sample [18]. The CL images display a uniform spatial distribution of threading dislocations at the surface as well as a uniform microstructure. CL images of the backside of the samples were similar to those of the front side. Corresponding scanning electron microscope images showed smooth planar surfaces. Both samples produced similar DR results. Because of the larger thickness, the Furukawa sample was used in the DT measurements.

III. RESULTS AND DISCUSSION

A. Differential transmission

Figure 1 shows DT transients measured at different degenerate pump-probe photon energies. The DT transients experience a rise, determined by the pulse width, and a rapid decay. At low photon energies, the DT decay is very fast; at higher energies, it becomes slower. Decay times for different photon energies, determined after deconvolution with a Gaussian pulse, are shown in Fig. 2. In the decay time spectrum, one can notice a clear threshold at 1.06 ± 0.02 eV.

First, let us discuss optical transitions that could produce an ultrafast transmission change and a threshold-like decay time spectrum. Transitions in the NIR can take place from deep centers related to defects and impurities (process 1, inset to Fig. 2), and within the conduction band via free electron absorption (process 2). The fast DT decay shows that the system relaxes to its initial state very rapidly. To achieve a subpicosecond electron relaxation to the deep levels in the case of process 1, the point defect concentration should be of the level of 10^{19} cm^{-2} [19, 20]. This is improbable for the low defect density GaN. Besides, cw transmission measurements in the spectral region from 0.82 eV to 1.65 eV showed a very weak absorption with a coefficient < 1

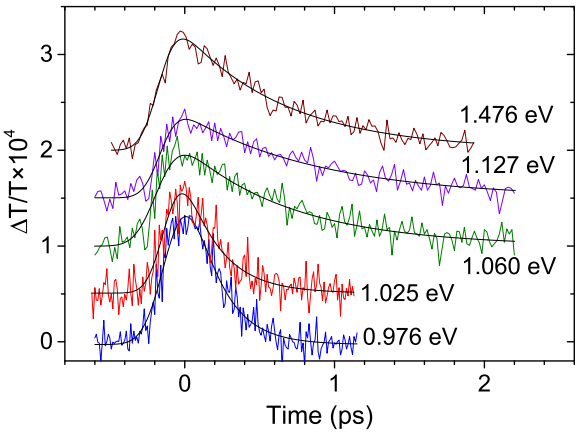

FIG. 1. (Color online). DT transients measured for different pump and probe photon energies. The black solid lines are fits with a convoluted function of a Gaussian peak and an exponential decay.

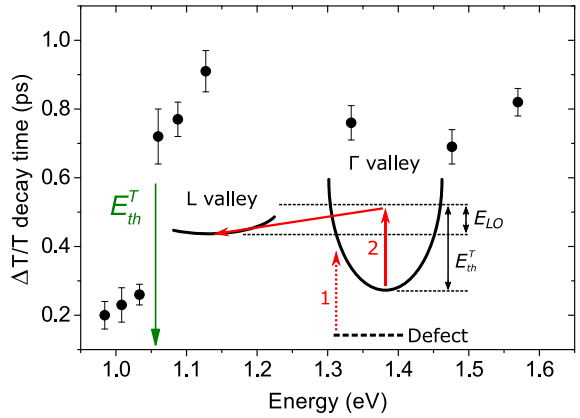

FIG. 2. (Color online). Spectrum of DT decay times. The inset shows schematics of transitions that can be induced by the pump pulses. 1− transitions from deep centers, 2− free electron absorption and intervalley electron scattering with an LO phonon emission.

cm^{-1}. Thus, the DT transients cannot be assigned to the deep level transitions; they should be attributed to the free electron transitions instead. Here one should note that a standard spectrometer, used in the linear transmission measurements, was not sensitive enough to detect transmission changes of the order of 1×10^{-4}; hence, the spectral step in the decay time spectrum (Fig. 2) could not be resolved. The weak free carrier absorption in the studied spectral range can be explained by the relatively short wavelengths (the free carrier absorption is roughly proportional to the squared wavelength) and the small absorption cross-section [21].

The free carrier absorption can be described by the Drude model, according to which the absorption coefficient α is proportional to the electron concentration N and the inverse effective mass $m_e^*, \alpha \propto N/m_e^*$ [22]. In the NIR DT measurements, the pump pulse does not change the electron concentration; consequently, the change in transmission reflects the change of the average effective mass of photoexcited electrons. For higher conduction band states, the electron effective mass is larger due to the nonparabolicity of the Γ valley [23] and the small dispersion of the L valley. Then, the short DT decay time at lower pump photon energies reflects the fast relaxation of hot Γ electrons towards the bottom of the valley. For excitation above 1.06 eV, the DT decay time is prolonged by the electron scattering to the L valley and back to the Γ valley. The intervalley scattering takes place primarily with participation of LO phonons, since the electron scattering time by large wave vector LO phonons is much smaller than that for corresponding acoustic phonons [24, 25]. At room temperature, the population of LO phonons is small, thus, scattering with a phonon emission is much more likely than with absorption [24]. Then, the measured threshold energy E_{th}^T corresponds to the sum of the IVE and the intervalley LO phonon energy (inset to Fig. 2),

$$E_{th}^T = E_{\Gamma-L}^T + E_{LO}. \quad (1)$$

For an intervalley LO phonon energy of 92 meV [26], the IVE is estimated as 0.97 ± 0.02 eV.

B. Differential reflection

To confirm this IVE value with an independent experiment, two color DR measurements were carried out. In general, the DR signal reflects changes induced by the pump pulse in the complex refractive index at the wavelength of the probe. For the interband and free carrier absorption, the real part of the refractive index dominates [27, 28]. Figure 3 shows normalized DR transients in the UV pump / IR probe configuration measured at different pump and probe photon energies at short times after the pump. The transients can be described by a double-exponential rise. The fast rise component, retrieved after deconvolution with the Gaussian pulse, is about 0.2 ps for the lower and 0.7 ps for the higher pump photon energies. The slower (and weaker) DR rise component, especially evident in the 4.25 eV transient, is about 1.5 ps for all pump photon energies. The DR signal decay (inset to Fig. 3) has two components with the shorter time of 32 ps and the longer one of ~ 800 ps.

Out of these four characteristic times, only the short rise time varies with the pump photon energy. Its spectrum is shown in Fig. 4. An abrupt increase takes place with a threshold at 4.67 ± 0.02 eV. Apart from the transition region, the rise time values remain fairly constant. Curiously, while the previous UV pump and IR probe study [13] determined the intervalley scattering threshold energy close to the one reported here (see below), the shape and the characteristic times of the DR transients were quite different from ours. In Ref. 13, the difference between transients for higher and lower pump photon energies is miniscule, and the higher energy DR rise times

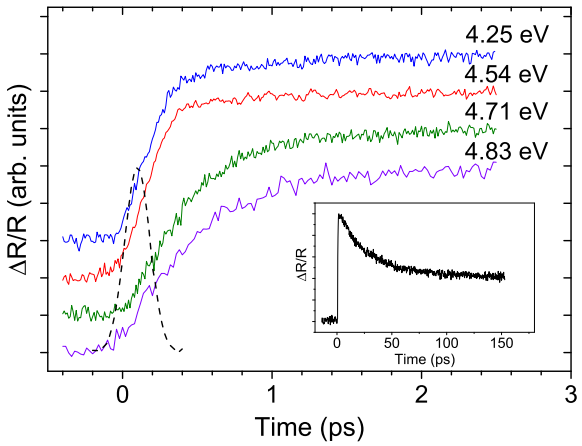

FIG. 3. (Color online). Normalized DR transients for different pump photon energies. The black dashed line shows autocorrelation trace of the pump pulse. The inset presents 4.54 eV transient measured on a long time scale.

are slightly shorter than those at the lower energies, contrary to our observation. Therefore, similarly as in the DT case, a careful analysis of transitions that may contribute to the DR should be performed before a definite conclusion about the origin of the step in the DR rise time spectrum can be drawn.

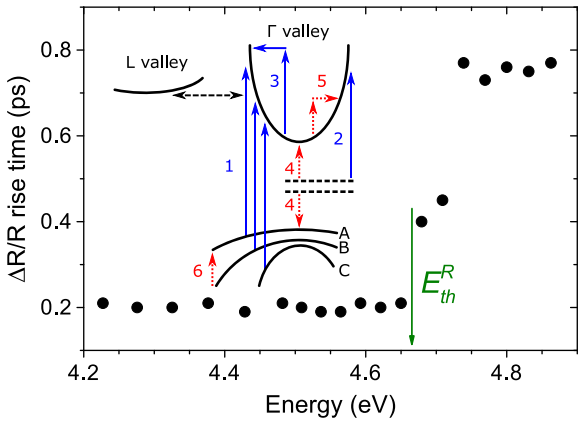

FIG. 4. (Color online). Spectrum of DR rise time and schematics of a GaN band structure with indicated optical transitions active under the excitation with pump (blue solid arrows) and probe (red dotted arrows) photons. These transitions are: (1) interband, (2) and (4) defect and impurity related, (3) and (5) free electron, and (6) intervallence band. The arrows depicting the optical transitions are not in scale.

In our DR experiment, the pump photon energies exceed the room temperature GaN band gap energy $E_g = 3.44$ eV [29] by 0.79 to 1.42 eV. For these excess energies, electrons can be excited into the Γ valley of the conduction band from valence bands A, B and C (transitions 1, inset to Fig. 4). For a small pump beam incidence angle, the light is polarized primarily $\boldsymbol{E} \perp \boldsymbol{c}$. According to the selection rules at $\boldsymbol{k} \approx 0$, for this polarization transitions from the band A are dominant [23]. Due to the lack of detailed information on the dependence of the selection rules on the $\boldsymbol{k}$ vector as well as on the density of states away from the Brillouin zone center, a quantitative evaluation of contributions of transitions from different valence bands to the DR signal is hardly possible. For this study, though, the most relevant parameter is the onset of the intervalley electron scattering. Assuming for a moment that the spectral step in the DR rise time is indeed related to the intervalley scattering, the threshold energy should be assigned to the lowest energy transitions, i.e. those originating from the valence band A, since for the other bands it would occur at higher energies.

Other optical transitions that can be excited by UV pulses are transitions from deep centers (2) and those of free electrons (3). Due to the weak absorption in the NIR, these transitions are 4 to 5 orders of magnitude weaker than the interband transitions. Hence, one can safely conclude that the interband absorption totally dominates optical transitions at the energies of the UV pump pulse.

In the experiment, the probe pulse wavelength is tuned along with that of the pump, hence, a possible impact of the probe absorption on the DR should also be explored. Dependence of the DR signal on the probe wavelength resembles that of PL excitation [30, 31], thus, absorption resonances in the NIR could provide features in the DR spectrum [32]. However, the cw transmission measurements have not revealed peaks around 1.55 eV (one third of the 4.65 eV pump photon energy) where the step in the DR rise time occurs. Thus, the step cannot be related to the defect/impurity (4) and free electron (5) transitions. As far as the intervalence band transitions (6) are concerned, the hole relaxation to the band A occurs on a 10-fs time scale [33], which is very different from the 800 ps DR decay time.

The long decay times, though, are characteristic for the interband recombination. Thus, the DR signal can with confidence be assigned to free carriers generated by the pump pulse via the interband absorption. The DR dynamics after the pulse are determined by the temporal evolution of the free carrier concentration and distribution in the bands. For photoexcited electron and hole concentrations N and P ($N = P$ for $N \gg N_0$, where N_0 is the DR signal is proportional to the differential refractive index $\Delta n/n$. Following the Drude model [34], it can be expressed as:

$$DR \propto \frac{\Delta n}{n} = \frac{2\pi e^2}{\varepsilon \omega^2}\left(\frac{N}{m_e^*} + \frac{P}{m_h^*}\right). \qquad (2)$$

Here, ε is the low frequency dielectric constant, ω is the light frequency and m_h^* is the hole effective mass. In GaN, the Γ valley electron effective mass is $0.22m_0$ [35], where m_0 is the free electron mass. For holes the data is scattered; the average literature value for the A band effective mass along the $\boldsymbol{c}$ axis is $1.58m_0$ [36]. Thus, even considering the uncertainty in the hole mass value, the

electron contribution to the DR signal should be dominant.

After the excitation high up in the conduction band, electrons thermalize between themselves within a few tens of fs, i.e. essentially during the pump pulse. Subsequently, the electron ensemble cools down, primarily via emission of LO phonons. The electron relaxation towards the bottom of the Γ valley is equivalent to the decrease of the average effective mass of the ensemble. During the first few picoseconds after the pump pulse, carrier recombination and diffusion may be neglected, and the photoexcited carrier density considered constant. Thus, following the Drude model (Eq. 2) and similarly to the DT case, the main increase of the DR signal should be assigned to the temporal change of the average effective mass of the electron ensemble.

Before proceeding to the analysis of the short DR rise time and its spectrum, let us briefly discuss the other DR rise and decay times. The slower DR rise component is most probably related to the relaxation of holes, since, according to Eq. 2, they also contribute to the change of the refractive index. The ratio between the amplitudes of the fast and slow DR rise components is ~ 7, close to the ratio of the hole and electron effective masses. Due to the much smaller hole excess energy obtained during the photoexcitation, emission of just one LO phonon transfers the hole population into a slower relaxation regime with emission of acoustic phonons. Following our interpretation, this slower relaxation towards the valence band region with a smaller mass has a characteristic time of 1.5 ps.

The short and long decay times of 32 and 800 ps should be attributed to the decrease of the electron concentration due to trapping and recombination. This assignment is based on the comparison with the time-resolved PL, the decay of which also has a double-exponential shape with similar decay times. The slow decay component can be assigned to the nonradiative recombination, since the radiative 300 K lifetime in GaN is of the order of tens of ns [37]. The fast decay component is excitation density dependent and disappears at high photoexcited carrier densities. Such a behavior is characteristic for trap saturation. PL does not allow distinguishing between electron and hole traps; however, the fact that a similar component is present in the DR transients dominated by the electron dynamics, allows assigning the fast decay component to the electron trapping. The capture process can take place in the bulk or at the surface. In n-GaN, shallow electron traps in the bulk are filled. Thus, the traps responsible for the short DR and PL decay times are most likely located at the surface. It has been shown that surface traps have a large impact on carrier dynamics in GaN [37].

Now, let us return to the discussion on the short DR rise time. Its step-like spectrum is similar to the DT decay time and shows that the rate of the electron relaxation towards the bottom of the conduction band is affected in a threshold-like manner. A sharp increase of the electron relaxation time occurs when the electron scattering between Γ and L valleys becomes possible. For pump photon energies corresponding to excited electron energies below the scattering threshold, electrons rapidly relax to the bottom of the Γ valley. Electrons excited into high conduction band states undergo scattering between the Γ and the L valleys before they reach the bottom of the conduction band.

To evaluate the IVE $E^R_{\Gamma-L}$ from the measured threshold energy for the intervalley scattering $E^R_{th} = 4.67 \pm 0.02$ eV, one should take into account conduction and valence band dispersion. The IVE is related to the experimental result via

$$E^R_{\Gamma-L} = E^R_{th} - E_g - E_{LO} - \Delta E_{vb}, \qquad (3)$$

where ΔE_{vb} is the excess hole energy in the valence band. In the parabolic band approximation with electron and hole effective masses of $0.22m_0$ and $1.58m_0$, respectively, $E^R_{\Gamma-L} = 1.00 \pm 0.02$ eV. The threshold energy measured by Wu *et al.* [13] is 4.53 ± 0.05 eV corresponding to the IVE of 0.87 ± 0.05 eV, which is rather close to our estimation. However, the nonparabolicity of the conduction [23] and valence bands [38] induces an uncertainty in the IVE that cannot be eliminated in the UV pump-IR probe DR experiment. In that sense, DT measurements, reported above, are more direct.

Nevertheless, the DR results are useful not only as a less accurate confirmation of the IVE determined by the DT. Comparison of the threshold energies determined by the DR and DT provides information on the valence band dispersion. The hole excess energy evaluated from Eq. 1 and 3 is $\Delta E_{vb} = E^R_{th} - E^T_{th} - E_g = 0.16$ eV. The electron excess energy of 1.06 eV (E^T_{th}) corresponds to the wave vector of $\sim$ 2.5 nm^{-1} with the conduction band nonparabolicity taken into account [23]. For that wave vector and the estimated E_{vb}, the band A hole mass in the parabolic band approximation is equal to $1.4m_0$. As discussed in Ref. [36], values of experimentally determined hole effective mass vary in a wide range, from $0.3m_0$ to $2.2m_0$, with an average value of $1.58m_0$. Our effective mass value is fairly close to this number. Theoretical calculations [39, 40] have also produced scattered values with an average of $1.7m_0$. One should mention that most of these effective masses were obtained for $\boldsymbol{k} \approx 0$, thus, a direct comparison with our value, estimated using the parabolic approximation for a large portion of the Brillouin zone, should be made with some reservation.

C. Modeling of reflection transients

Apart from providing the IVE, the DR dynamics allow estimating intervalley scattering times. To that end, the DR transients were modeled with rate equations in which continua of conduction band states at different energies are simplified by discrete energy levels (inset to Fig. 5). The basis of the model is the four level system developed for GaAs [41] and modified for pump-probe experiments

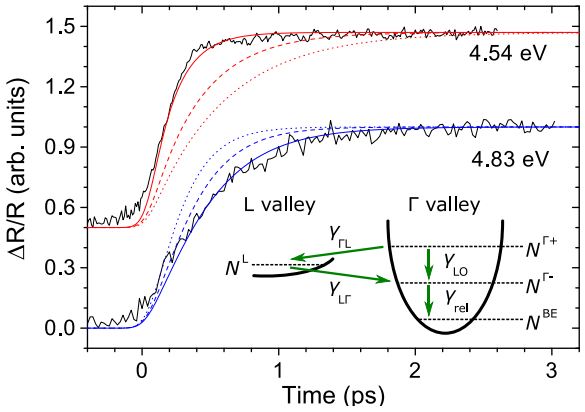

FIG. 5. (Color online). Experimental and simulated DR curves for pump photon energies below (4.54 eV) and above (4.83 eV) the intervalley scattering threshold. The inset shows levels and scattering rates described in Eq. 4-9. For the 4.54 eV transient, the red solid line correspond to $1/\gamma_{LO} = 30$ fs, the red dashed line - 60 fs, the red dotted line - 90 fs. The blue solid line correspond to $1/\gamma_{L\Gamma}$ of 360 fs ($m_L/m^*_{\Gamma+} = 4$), the blue dashed line - 230 fs (3), the blue dotted line - 130 fs (2).

by taking into account the temporal profile of the pump pulse [13]. Different levels are assigned to the states in the Γ valley above (Γ^+) and below (Γ^-) the intervalley scattering threshold, and the states in the L valley (inset to Fig. 5). To take into account the conduction band nonparabolicity, a fourth level Γ^{BE}, corresponding to states close to the bottom of the conduction band, is introduced, since these lighter mass states contribute to the major part of the DR signal. In addition, our model differs from that of Ref. 41 in that electron scattering from the L valley with LO phonon emission can take place only to the Γ^- state. The four level rate equations for excitation above the intervalley scattering threshold are then defined as follows:

$$\frac{dN^{\Gamma+}}{dt} = \frac{I(t)\alpha}{h\nu} - (\gamma_{\Gamma L} + \gamma_{LO})N^{\Gamma+}(t) \tag{4}$$

$$\frac{dN^{L}}{dt} = \gamma_{\Gamma L}N^{\Gamma+}(t) - \gamma_{L\Gamma}N^{L}(t) \tag{5}$$

$$\frac{dN^{\Gamma-}}{dt} = \gamma_{LO}N^{\Gamma+}(t) - \gamma_{rel}N^{\Gamma-}(t) + \gamma_{L\Gamma}N^{L}(t) \tag{6}$$

$$\frac{dN^{BE}}{dt} = \gamma_{rel}N^{\Gamma-}(t) \tag{7}$$

For excitation below the threshold, only the relaxation to the bottom of the Γ valley has to be considered:

$$\frac{dN^{\Gamma-}}{dt} = \frac{I(t)\alpha}{h\nu} - \gamma_{rel}N^{\Gamma-}(t) \tag{8}$$

$$\frac{dN^{BE}}{dt} = \gamma_{rel}N^{\Gamma-}(t) \tag{9}$$

The term $I(t)\alpha/h\nu$ stands for the carrier generation by an optical pulse with a power density of $I(t)$ and a photon energy of $h\nu$. N is the electron concentration at a particular level, and $\gamma_{\Gamma L}$, $\gamma_{L\Gamma}$ and γ_{LO} are the rates of the electron scattering between levels $\Gamma^+ \to$ L, L $\to \Gamma^-$,and $\Gamma^+ \to \Gamma^-$, respectively. All these processes take place with participation of LO phonons with inter- and intravalley wave vectors. The rate γ_{rel} reflects electron relaxation to the bottom of the Γ valley. The Γ valley dispersion shows that the nonparabolicity becomes important at electron excess energies of ~ 0.5 eV [23]. Hence, in our simple model we consider that it takes 6 intravalley LO phonons for an electron in the Γ^- state to reach the parabolic part of the Γ valley, i.e. $\gamma_{rel} = \gamma_{LO}/6$. Our results show that $\gamma_{\Gamma L}$ must be larger than γ_{LO}, otherwise electrons for the above threshold excitation would immediately relax to the Γ^- state and we would not observe the slow rise of the DR signal. Due to lack of available data for GaN, we will assume $\gamma_{\Gamma L} = 4\gamma_{LO}$ as for GaAs [41].

Phonon-assisted intervalley scattering rate of electrons from the initial ith valley with energy ε to the jth valley is given by [42]:

$$\gamma_{ij} = \frac{D_{ij}^2 Z_j m_j^{3/2}}{\sqrt{2}\pi\hbar^3\rho\omega_i j}[(N_{ij}+1)(\varepsilon - \hbar\omega_{ij} - \varepsilon_{0j})^{1/2} + N_{ij}(\varepsilon + \hbar\omega_{ij} - \varepsilon_{0j})^{1/2}]. \tag{10}$$

Here D_{ij} is the deformation potential between the ith and jth valleys, Z_j is the degeneracy and m_j is the effective mass of electrons in the jth valley, ρ is the density of the crystal, ω_{ij} is the phonon energy for the $i \to j$ intervalley scattering, N_{ij} is the number of intervalley scattering phonons, and, finally, ε_{0j} is the energy at the bottom of the jth valley. The first and the second terms in the angular brackets represent transitions with a phonon emission and absorption, respectively. In the case of only two valleys, γ_{ij} and γ_{ji} rates are related via the detailed balance and are proportional to the equilibrium ratio (R) of the valley populations [41]. From Eq. 10 one can express this ratio via electron effective masses and degeneracy factors of Γ and L valleys,

$$R = \frac{\gamma_{\Gamma L}}{\gamma_{L\Gamma}} \propto \frac{Z_L}{Z_\Gamma}\left(\frac{m_L^*}{m_{\Gamma+}^*}\right)^{3/2}. \tag{11}$$

Taking into account the six-fold degeneracy of the L valley [43], we can solve the system of rate equations (4-7) by varying the ratio between effective masses in the Γ^+ and L states. Here one should remember that $m^*_{\Gamma+}$ is considerably larger than the electron effective mass at the Γ band-edge (at $\boldsymbol{k} = 2.5$ nm^{-1} $m^*_\Gamma \approx 0.4m_0$ [23]).

The simulation results are shown in Fig. 5. The upper curves, corresponding to the pump photon energy below the intervalley scattering threshold, are mainly affected by the LO phonon emission time. The best fit is obtained for the value of 30 fs. Literature values of the intravalley electron - LO phonon scattering time vary in a broad range, from 13 fs [44] to 290 fs [13]. The value obtained in our simulations falls into the lower end of this range. The curves for the above-threshold excitation are calculated by taking $1/\gamma_{LO} = 30$ fs, $1/\gamma_{\Gamma L} = 7.5$ fs and varying $m_L^*/m_{\Gamma+}^*$. Here, the best fit is obtained for $m_L^*/m_{\Gamma+}^* = 4$, which gives $R = 48$ ($1/\gamma_{L\Gamma}$ of 360 fs). The maximal fraction of electrons transfered to the L valley is estimated at 60%. This relatively low value can be explained by the fast electron relaxation in the Γ valley. A certain discrepancy between the experimental and the calculated DR transients can be ascribed to the relaxation of holes, which was not considered in the model.

IV. CONCLUSIONS

In conclusion, time-resolved transmission and reflection measurements were performed for bulk GaN in order to evaluate the energy of the first satellite valley above the minimum of the conduction band. The measurements showed clear threshold-like spectra for DT decay and DR rise times, which were associated with the onset of the intervalley electron scattering. The wavelength degenerate transmission measurements with pulses in the near IR have produced the intervalley energy of 0.97 ± 0.02 eV. The UV pump and IR probe reflection measurements provided a similar value. Comparison of the DT and DR threshold energies allowed estimating the hole effective mass in the upper-most band as $1.4m_0$. Modelling of the reflection transients with rate equations showed that electron - LO phonon scattering time is about 30 fs for the intravalley and 8 fs for the intervalley scattering.

ACKNOWLEDGMENTS

Research at KTH was performed within the frame of Linnaeus Excellence Center for Advanced Optics and Photonics (ADOPT), and was financially supported by the Swedish Research Council (Contract No. 621-2013-4096).Research at UCSB was supported in part by the Department of Energy (program DE-EE0007096) and by the KACST-KAUST-UCSB Solid State Lighting Program.

* sm@kth.se

[1] J. Iveland, L. Martinelli, J. Peretti, J. S. Speck, and C. Weisbuch, Phys. Rev. Lett. **110**, 177406 (2013).
[2] M. Piccardo, L. Martinelli, J. Iveland, N. Young, S. P. DenBaars, S. Nakamura, J. S. Speck, C. Weisbuch, and J. Peretti, Phys. Rev. B **89**, 235124 (2014).
[3] M. Semenenko, O. Yilmazoglu, H. L. Hartnagel, and D. Pavlidis, J. Appl. Phys. **109**, 023703 (2011).
[4] K. T. Delaney, P. Rinke, and C. G. Van de Walle, Appl. Phys. Lett. **94**, 191109 (2009).
[5] L. C. de Carvalho, A. Schleife, and F. Bechstedt, Phys. Rev. B **84**, 195105 (2011).
[6] M. Rakel, C. Cobet, N. Esser, F. Fuchs, F. Bechstedt, R. Goldhahn, W. G. Schmidt, and W. Schaff, Phys. Rev. B **77**, 115120 (2008).
[7] R. Goldhahn, K. Lange, and M. Feneberg, in *Proc. SPIE*, Vol. 9363 (2015) p. 93630G.
[8] C. Cobet, R. Goldhahn, W. Richter, and N. Esser, Phys. Stat. Sol. (b) **246**, 1440 (2009).
[9] D. E. Aspnes, M. Cardona, V. Saile, M. Skibowski, and G. Sprüssel, Solid State Commun. **31**, 99 (1979).
[10] N. Nepal, K. B. Nam, J. Li, M. L. Nakarmi, J. Y. Lin, and H. X. Jiang, Appl. Phys. Lett. **88**, 261919 (2006).
[11] F. Gütle, V. M. Polyakov, M. Baeumler, F. Benkhelifa, S. Müller, M. Dammann, M. Cäsar, R. Quay, M. Mikulla, J. Wagner, *et al.*, Semicond. Sci. Technol. **27**, 125003 (2012).
[12] C.-K. Sun, Y.-L. Huang, S. Keller, U. K. Mishra, and S. P. DenBaars, Phys. Rev. B **59**, 13535 (1999).
[13] S. Wu, P. Geiser, J. Jun, J. Karpinski, D. Wang, and R. Sobolewski, J. Appl. Phys. **101**, 43701 (2007).
[14] M. C. Nuss, D. H. Auston, and F. Capasso, Phys. Rev. Lett. **58**, 2355 (1987).
[15] J. Shah, IEEE J. Quantum Electron. **24**, 276 (1988).
[16] W. B. Wang, N. Ockman, M. Yan, and R. R. Alfano, Solid State Electron. **32**, 1337 (1989).
[17] A. David and M. J. Grundmann, Appl. Phys. Lett. **97**, 033501 (2010).
[18] H. M. Foronda, A. E. Romanov, E. C. Young, C. A. Roberston, G. E. Beltz, and J. S. Speck, J. Appl. Phys. **120**, 035104 (2016).
[19] A. Pinos, S. Marcinkevičius, M. Usman, and A. Hallén, Appl. Phys. Lett. **95**, 2108 (2009).
[20] T. K. Uždavinys, S. Marcinkevičius, J. H. Leach, K. R. Evans, and D. C. Look, J. Appl. Phys. **119**, 215706 (2016).
[21] P. Ščajev, K. Jarašiūnas, Ü. Özgür, H. Morkoç, J. Leach, and T. Paskova, Appl. Phys. Lett. **100**, 022112 (2012).
[22] J. Hebling, M. C. Hoffmann, H. Y. Hwang, K.-L. Yeh, and K. A. Nelson, Phys. Rev. B **81**, 035201 (2010).
[23] S. Shokhovets, O. Ambacher, B. K. Meyer, and G. Gobsch, Phys. Rev. B **78**, 035207 (2008).
[24] S. Shishehchi, S. Rudin, G. A. Garrett, M. Wraback, and E. Bellotti, J. Appl. Phys. **114**, 233106 (2013).
[25] G. Kokolakis, F. Compagnone, A. Di Carlo, and P. Lugli, Phys. Status Solidi A **195**, 618 (2003).
[26] J. C. Cao and X. L. Lei, Eur. Phys. J. B **7**, 79 (1999).
[27] M. Wraback and H. Shen, in *Proc. SPIE*, Vol. 4650 (2002) pp. 84–93.
[28] M. Soltani and R. Soref, Opt. Express **23**, 24984 (2015).
[29] B. Monemar, P. P. Paskov, J. P. Bergman, A. A. Toropov, T. V. Shubina, T. Malinauskas, and A. Usui, Phys. Status Solidi B **245**, 1723 (2008).

[30] A. V. Kuznetsov, C. S. Kim, and C. J. Stanton, J. Appl. Phys. **80**, 5899 (1996).
[31] V. Emiliani, T. Guenther, C. Lienau, R. Nötzel, and K. H. Ploog, J. Microsc. **202**, 229 (2001).
[32] W. B. Wang, K. Shum, R. R. Alfano, D. Szmyd, and A. J. Nozik, Phys. Rev. Lett. **68**, 662 (1992).
[33] R. Binder, D. Scott, A. E. Paul, M. Lindberg, K. Henneberger, and S. W. Koch, Phys. Rev. B **45**, 1107 (1992).
[34] M. C. Downer and C. V. Shank, Phys. Rev. Lett. **56**, 761 (1986).
[35] M. Drechsler, D. M. Hofmann, B. K. Meyer, T. Detchprohm, H. Amano, and I. Akasaki, Japan. J. Appl. Phys. **34**, L1178 (1995).
[36] B. Šantić, Semicond. Sci. Technol. **18**, 219 (2003).
[37] P. Ščajev, K. Jarašiūnas, S. Okur, Ü. Özgür, and H. Morkoç, J. Appl. Phys. **111**, 023702 (2012).
[38] P. A. Shields, R. J. Nicholas, F. M. Peeters, B. Beaumont, and P. Gibart, Phys. Rev. B **64**, 081203 (2001).
[39] D. Fritsch, H. Schmidt, and M. Grundmann, Phys. Rev. B **67**, 235205 (2003).
[40] A. Punya and W. R. L. Lambrecht, Phys. Rev. B **85**, 195147 (2012).
[41] C. J. Stanton and D. W. Bailey, Phys. Rev. B **45**, 8369 (1992).
[42] C. Herring, Bell System Technical Journal **34**, 237 (1955).
[43] U. V. Bhapkar and M. S. Shur, J. Appl. Phys. **82**, 1649 (1997).
[44] C. K. Choi, Y. H. Kwon, J. S. Krasinski, G. H. Park, G. Setlur, J. J. Song, and Y. C. Chang, Phys. Rev. B **63**, 115315 (2001).